JOURNAL OF BACTERIOLOGY, Apr. 1997, p. 2623–2631
0021-9193/97/$04.00+0

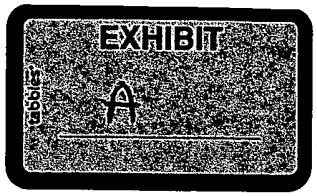

Vol. 179, No. 8

Cytochrome c_y of *Rhodobacter capsulatus* Is Attached to the Cytoplasmic Membrane by an Uncleaved Signal Sequence-Like Anchor

HANNU MYLLYKALLIO,[1] FRANCIS E. JENNEY, JR.,[1]† CAROLYN R. MOOMAW,[2] CLIVE A. SLAUGHTER,[2] AND FEVZI DALDAL[1]*

Department of Biology, Plant Science Institute, University of Pennsylvania, Philadelphia, Pennsylvania 19104-6018,[1] and Howard Hughes Medical Institute, Dallas, Texas 75235-9050[2]

Received 11 November 1996/Accepted 5 February 1997

During the photosynthetic growth of *Rhodobacter capsulatus*, electrons are conveyed from the cytochrome (cyt) bc_1 complex to the photochemical reaction center by either the periplasmic cyt c_2 or the membrane-bound cyt c_y. Cyt c_y is a member of a recently established subclass of bipartite *c*-type cytochromes consisting of an amino (N)-terminal domain functioning as a membrane anchor and a carboxyl (C)-terminal domain homologous to cyt *c* of various sources. Structural homologs of cyt c_y have now been found in several bacterial species, including *Rhodobacter sphaeroides*. In this work, a C-terminally epitope-tagged and functional derivative of *R. capsulatus* cyt c_y was purified from intracytoplasmic membranes to homogeneity. Analyses of isolated cyt c_y indicated that its spectral and thermodynamic properties are very similar to those of other *c*-type cytochromes, in particular to those from bacterial and plant mitochondrial sources. Amino acid sequence determination for purified cyt c_y revealed that its signal sequence-like N-terminal portion is uncleaved; hence, it is anchored to the membrane. To demonstrate that the N-terminal domain of cyt c_y is indeed its membrane anchor, this sequence was fused to the N terminus of cyt c_2. The resulting hybrid cyt *c* (MA-c_2) remained membrane bound and was able to support photosynthetic growth of *R. capsulatus* in the absence of the cyt c_y and c_2. Therefore, cyt c_2 can support cyclic electron transfer during photosynthetic growth in either a freely diffusible or a membrane-anchored form. These findings should now allow for the first time the comparison of electron transfer properties of a given electron carrier when it is anchored to the membrane or is freely diffusible in the periplasm.

Rhodobacter species are purple, nonsulfur, gram-negative facultative phototrophs with a wide variety of growth modes, including aerobic and anaerobic respiration and photosynthesis (Ps) (30). Consequently, their electron transport chains are highly branched and constitute a model system for the study of microbial and organelle energy transduction (10). In these bacteria, Ps relies on cyclic electron transfer between the photochemical reaction center (RC) and the ubihydroquinone: cytochrome (cyt) c_2 oxidoreductase (cyt bc_1 complex). Transfer of electrons between these membrane-bound complexes is mediated by the quinone pool in the lipid bilayer and by periplasmic or membrane-bound *c*-type cytochromes outside the membrane (18). The electrochemical proton gradient thus produced is used for ATP synthesis, transport, and various forms of taxis (10).

In wild-type *Rhodobacter sphaeroides*, cyclic electron transfer depends strictly on the presence of the periplasmic cyt c_2 (8), while in *Rhodobacter capsulatus*, Ps growth occurs in the absence of cyt c_2 (6) because of the presence of the membrane-bound cyt c_y (encoded by *cycY*) (18). In a wild-type *R. capsulatus* strain like MT-1131 (Table 1), Ps electron transfer pathways mediated by both the cytochromes (c_2 and c_y) are active simultaneously (19), and both of these cytochromes can also reduce the cbb_3-type cyt *c* oxidase of this species (14) during respiratory growth (15). In addition, a functional *R. capsulatus* cyt c_y can be introduced genetically into *R. sphaeroides*, where it is able to support Ps growth in the absence of endogenous cyt c_2 (20). Recently, homologs of cyt c_y have been encountered in various species, including *Bradyrhizobium japonicum* (4), *Paracoccus denitrificans* (43), and *R. sphaeroides* (49). However, that of *R. capsulatus* is unique among the members of this newly described subclass of membrane-attached *c*-type cytochromes in that it operates in both Ps and respiration (15, 19).

Previous genetic and biochemical studies established that the monoheme cyt c_y is composed of two domains: the carboxyl (C)-terminal cyt *c* domain (highly homologous to those of mitochondrial cyts *c*) and its amino (N)-terminal extension of approximately 100 amino acids (18) (see Fig. 1 and 3). The latter domain can be further subdivided into a proximal signal sequence-like hydrophobic anchor subdomain followed by a linker subdomain rich in proline and alanine residues. While the role of the cyt *c* domain in electron transfer is obvious, the function of the N-terminal domain is less clear. It has been proposed that the lack of processing of the signal-like subdomain may cause it to serve as a membrane anchor of cyt c_y (18) and its homologs (4), but this proposal has remained untested until this work. Thus, to define in detail the physicochemical properties of *R. capsulatus* cyt c_y and to understand how it is attached to the cytoplasmic membrane, we have undertaken its purification. Here we describe the isolation and characterization of its biologically active, C-terminally epitope-tagged derivative (FLAGed cyt c_y). The data indicate that the redox midpoint potential ($E_{m,7}$) and optical spectra of purified cyt c_y are very similar to those of the soluble cyt c_2 and correspond closely to its in situ properties determined previously (19, 33).

* Corresponding author. Mailing address: Department of Biology, Plant Science Institute, University of Pennsylvania, Philadelphia, PA 19104-6018. Phone: (215) 898-4394. Fax: (215) 898-8780. E-mail: fdaldal@sas.upenn.edu.

† Present address: Department of Biochemistry, Center for Metalloenzyme Studies, University of Georgia, Athens, GA 30602-7229.

TABLE 1. Bacterial strains, phages, and plasmids used

Strain	Genotype	Phenotype	Reference
E. coli			
CJ236	*dut-1 ung-1 thi-1 relA1*/pCJ105 (F' Cam^r)	Dut$^-$ Ung$^-$	36
HB101	F$^-$ *proA2 hsdS20* (r_B^- m_B^-) *recA13 ara-14 lacY1 galK2 rpsL20 supE44 rpsL20 supE44 proA2 xyl-5 mtl-1*		36
XL1-Blue	*recA1 endA1 gyrA96 thi-1 hsdr-17 supE44 relA1 lac*[F' *proAB lacI^q* ΔM15 Tn*10*(Tet^r)]		Stratagene
CC118	*phoAΔ20 recA1*	PhoA$^-$	25
R. capsulatus			
MT-1131[a]	*crtD121* Rif^r	Wild type	39
Y262		GTA overproducer	47
FJ2	*crtD121* Δ(*cycA*::*kan*) Δ(*cycY*::*spe*)	cyt c_2^- c_y^-, Ps$^-$	18
FJ5	*crtD121* Δ(*MluI*/*Eco*RV::*spe*)	Lacks *MluI*/*Eco*RV fragment of pFJ6, PheA$^-$	This work
FJ6	*crtD121* Δ(*MluI*/*Eco*RV::*spe*) Δ(*cycA*::*kan*)	cyt c_2^- derivative of FJ5	This work
R. sphaeroides			
Gadc$_2$	*crt* Δ(*cycA*::*spe*)	Spe^r, cyt c_2^-, Ps$^-$	5
Phages			
λTn*phoA*	λ28(*b221 cI857 Pam3*)	Tn*phoA*	25
VCSM13	Kan^r	Helper phage	Stratagene
Plasmids			
pRK2013		Kan^r, helper	7
pRK415		Tet^r	7
pRK404		Tet^r	7
pBSII	pBluescriptII (KS+)	Amp^r	Stratagene
pFJ6	*cycY* on 6-kb *Bam*HI insert	Tet^r	18
pSH3	*R. capsulatus cycA* in pUC8	Amp^r	5
pXCA601	*lacZ*	Tet^r	1
pFJ631	1.2-kb *Bam*HI/*Hin*dIII fragment of pHM1 on pRK415	Tet^r CycY	This work
pHM1	1.2-kb *Bam*HI/*Hin*dIII fragment of pFJ61 in *Eco*RV site of pBSII	Amp^r CycY	18; this work
pHM2	1.25-kb *Sal*I/*Hin*dIII fragment of pSH3 in pBSII	Amp^r	This work
pHM3	Like pHM1 but contains *Eco*RI site at position 408	Amp^r	This work
pHM4	0.8-kb *Eco*RI fragment of pHM2 ligated to 3.4-kb *Eco*RI fragment of pHM3	Amp^r, cyt MA-c_2	This work
pHM5	0.8-kb *Eco*RI fragment of pHM3 ligated to 3.4-kb *Eco*RI fragment of pHM2	Amp^r	This work
pHM6	Like pHM1 but contains FLAGed allele of *cycY*	Amp^r, FLAGed cyt c_y	This work
pHM7	pHM6 at *Bam*HI site of pRK415	Amp^r Tet^r, FLAGed cyt c_y	This work
pHM8	1.2-kb *Kpn*I/*Bam*HI fragment of pHM4 on pRK415	Tet^r, cyt MA-c_2	This work
pHM9	1.2-kb *Kpn*I/*Bam*HI fragment of pHM5 on pRK415	Tet^r, cyt S-c_y	This work
pHM10	*cycY49*::*phoA*	Cyt c_y::*phoA* fusion at position 49, Tet^r Kan^r	This work
pHM11	*cycY188*::*phoA*	Cyt c_y::*phoA* fusion at position 188, Tet^r Kan^r	This work
pHM12	*PcycY*::*lacZ* in pXCA601	Tet^r	1; this work
pA53C404	*cycY* with A53C mutation on pRK404	Tet^r Amp^r	This work
pA89C404	*cycY* with A89C mutation on pRK404	Tet^r Amp^r	This work
pA260C404	*cycY* with A260C mutation on pRK404	Tet^r Amp^r	This work

[a] *R. capsulatus* MT-1131 (Rif^r *crtD*) is referred to as wild type, since it is wild type with respect to its cytochrome *c* profile and growth properties. MT-1131 was originally isolated as a green derivative of *R. capsulatus* SB1003 (39).

Moreover, purified mature cyt c_y still contains its N-terminal signal sequence-like extension, indicating that it remains attached to the membrane because of its lack of processing. Finally, we demonstrate that the N-terminal domain of cyt c_y can also anchor to the membrane the periplasmic cyt c_2 in a biologically active form. Therefore, both the soluble and the membrane-bound forms of this electron carrier are able to support Ps growth of *R. capsulatus*.

MATERIALS AND METHODS

Bacterial strains and growth conditions. The bacterial strains and plasmids used in this work are described in Table 1. *R. capsulatus* and *R. sphaeroides* strains were grown under chemoheterotrophic or photoheterotrophic conditions in enriched medium (MPYE) or in Sistrom's minimal medium A (Med A) (18, 40). Photoheterotrophic growth on solid media used anaerobic jars and H_2- and CO_2-generating gas packs from BBL. Cyt c_y was purified from cells grown semiaerobically in a mixed medium composed of 50% Med A and 50% MPYE, which yields a higher biomass (14). *Escherichia coli* strains were grown on Luria broth (LB medium), and cultures were supplemented with appropriate antibiotics for plasmid selection and maintenance as described earlier (6, 18).

Molecular genetic techniques. Standard molecular genetic techniques were as described earlier (18, 36). For site-directed mutagenesis of *cycY*, uracilated single-stranded DNA was isolated from *E. coli* CJ236 containing pHM1 (Table 1). Infection of pHM1/CJ236 with the helper phage VCSM13, isolation of single-stranded DNA, and site-directed mutagenesis were performed according to the manufacturer's instructions (Stratagene). In the mutagenic primers CYM1 (5'-TTG GCG CAG CTA CGC GCT-3'), CYM2 (5'-GAC GAG CAG GGC TCC

CCC-3'), and CYM3 (5'-GGC GGG CAG GGC GGC CTC-3') leucine replaced methionine residues 1, 13, and 70 of *cycY* (numbering refers to the amino acid positions of ORF1, part of which encodes cyt c_y) (GenBank accession number, Z21797; 18). The mutagenic primer 5'-CTG CAG CTG CGC TCA CTT GTC ATC GTC GTC CTT GTA GTC GCG CGG CAG CGT GTT CAG-3' extended the C terminus of cyt c_y with an in-frame octapeptide (N-Asp Tyr Lys Asp Asp Asp Lys-C), which corresponds to the FLAG epitope (Scientific Imaging Systems, Kodak) followed by a stop codon.

The plasmid pHM2 carries *R. capsulatus cycA* in a 1.25-kb *Sall/Hin*dIII fragment and contains an *Eco*RI site at position 454 of the insert, corresponding to glutamic acid 8 of mature cyt c_2 (Table 1). By using the mutagenic primer 5'-CTT GTT GAA TTC CTT CTC GCC GGC TTT CGC-3', an *Eco*RI restriction site which inverted the order of the glutamic acid 105 and lysine 106 of cyt c_y was introduced by site-directed mutagenesis into *cycY* and yielded pHM3. These *Eco*RI sites were then used to swap the cyt domains of the cytochromes c_2 and c_y by ligating together, in the appropriate orientation, the 0.8- and 3.4-kb *Eco*RI fragments of pHM2 and pHM3. These constructions yielded plasmids pHM4 and pHM5, which carry hybrid cytochromes formed of the N-terminal domain of cyt c_y fused to cyt c_2 (cyt MA-c_2) and the signal sequence of cyt c_2 fused to the cyt *c* domain of cyt c_y (cyt S-c_y) (Table 1). All constructs were subsequently confirmed by DNA sequencing.

DNA sequence analysis. DNA sequence analysis of the region surrounding *cycY* was done initially by manual sequencing, using α-^{35}S-ATP and a USB Sequenase kit (18). Later on, automated sequencing and a dye terminator cycle sequencing kit (Amplitaq FS) from Applied Biosystems were used as specified by the manufacturer. Various subclones of pFJ6 (18) were used as single-stranded DNA templates with the following primers (shown in 5'-to-3' orientation) synthesized at DNA Synthesis Service, Department of Chemistry, University of Pennsylvania: BE30, TGCTCGTCGAGGATATGCAG; FR6, CGATGATGCT TTCGATC; BE26, TCGAGGCGGCCAGTTCCG; FR7, CATTGCGGCACCC AGAA; FF5, GGGCGAGGCCTATTGCC; FR8, CGCATCATCGACGCGCA; FF6, CGATTACCCGAAGCGCG; HM20, CTACATGCTTGACGGCT; FF7, CAGCTACACGTTCCGCA; HM38, CCTATTCGCACGAGGCCGC; FR3, G GCGCCTTGGGGGGCAT; HM50, TGTGCGGGCGCATCTGG; FR5, CAC CAGATCGACCACCG.

DNA analyses, predictions for segmental flexibility in amino acid sequences, and homology searches were done using MacVector (IBI, Kodak) and BLAST programs (2). The computer programs TmPred (16) and Clustal W (42) were used to predict the positions of the transmembrane helixes and to align sequences, respectively.

Construction of the *cycY::lacZ* fusion. A *cycY::lacZ* fusion was constructed by PCR cloning of the 0.2-kb *pheA-cycY* intergenic region into the conjugative promoter-probe vector pXCA601 containing an in-frame *Bam*HI site at the 5' end of *lacZ* (1). Briefly, this region was amplified by *Taq* DNA polymerase with 200 ng of the primers TF1 (5'-GCC CTG CAG GCA TTC CCC TGA CAG TCG-3') and TF2 (5'-CCC GGA TCC GTG ATG TGC GTC TTG ACG AGC-3') in the presence of 20 ng of pFJ6 as DNA template, 10 mM Tris-HCl, 1.5 mM $MgCl_2$, 75 mM KCl, and a 50 μM concentration of each deoxynucleoside triphosphate. The reaction mixture was incubated at 98°C for 30 s prior to cycling (30 cycles of 97°C for 30 s, 55°C for 10 s, and 72°C for 60 s), and the PCR product thus obtained was digested with *Pst*I and *Bam*HI restriction enzymes and cloned into the corresponding sites of pXCA601. The resulting plasmid, pHM12, carried a DNA fragment of 215 bp extending from the translational start site of *pheA* to the threonine 8 of cyt c_y and yielded an in-frame *cycY::lacZ* translational fusion.

Isolation of *cycY::phoA* fusions. Transposition of Tn*phoA* from phage λ128 (*b*221 *c*I857 *P*am3) into pFJ631 carrying *cycY* was used to isolate *cycY::phoA* fusions as described previously (25, 38). Plasmid DNA was extracted from a pool of Kan^r colonies obtained by infection of pFJ631/CC118 with λ128 and retransformed into HB101 selecting for Kan^r. The resulting population was used as a donor in a triparental cross into the Ps$^-$ *R. sphaeroides* strain Gadc$_2$ (cyt c_2^-) with selection under respiratory growth conditions for Kan^r on Med A plates containing XP (5-bromo-4-chloro-3-indolylphosphate). Blue colonies thus obtained were tested for their abilities to grow under Ps conditions, and those that were Kan^r Tet^r Ps$^-$ were analyzed by restriction digestion. The exact locations of the Tn*phoA* insertions in *cycY* were determined by DNA sequencing with the oligonucleotide 5'-GCC GGG TGC AGT AAT ATC G-3' complementary to positions 80 to 98 of *phoA*.

Chromosomal inactivation of the upstream region of *cycY*. The 0.9-kb *Eco*RV/*Mlu*I fragment located immediately upstream of *cycY* was deleted from pFJ6 and replaced by the polar Spe^r Ω cartridge (18). The resulting deletion-insertion mutation was introduced into the chromosomes of *R. capsulatus* MT-1131 (wild type) and MT-G4/S4 (cyt c_2^-) by using a gene transfer agent (47) as described previously, yielding FJ5 and FJ6, respectively.

Isolation of chromatophore vesicles and membrane sheets. Intracytoplasmic membrane vesicles (chromatophores) were prepared by using a French press (SLM Aminco) as described previously (14) in the presence of the protease inhibitors Pefabloc SC, leupeptin, and Pepstatin A as recommended by the manufacturer (Boehringer Mannheim, Mannheim, Germany). Membrane sheets were isolated from lysozyme-treated cells (21) by osmotic lysis in 10 mM K_2PO_4 (pH 7.4)–2 mM EDTA–0.1 mM phenylmethylsulfonyl fluoride (PMSF) buffer. Once the lysis was complete, catalytic amounts of DNAse (Boehringer Mannheim) and 10 mM $MgCl_2$ were added, and mixing continued for 60 min at 4°C. Membrane sheets were isolated by centrifugation at 25,000 × *g* for 20 min and washed once in the above-described buffer. To distinguish between peripheral and integral membrane proteins, membrane fragments were then incubated either with 1 M NaBr or with 100 mM 3-(cyclohexylamino)-1-propane sulfonic acid (CAPS)-NaOH (pH 10.5) on ice for 30 min, diluted 40-fold with 30 mM Tris-HCl (pH 8.0)–5 mM EDTA–0.1 mM PMSF–20% glycerol, reisolated by centrifugation at 150,000 × *g* for 20 min, and washed once. Supernatants containing peripheral membrane proteins (after concentration using a 3-kDa cutoff filter [Amicon]) and pellets containing integral membrane proteins were subsequently analyzed by sodium dodecyl sulfate-polyacrylamide gel electrophoresis (SDS-PAGE). Protein assays were done by the method of Lowry et al. (23), with bovine serum albumin as a standard.

Purification of FLAGed cyt c_y. An epitope-tagged derivative of cyt c_y (FLAGed cyt c_y) was purified from chromatophores of pHM7/FJ2 (Table 1), and all manipulations were performed at 4°C. Chromatophore membranes were solubilized with 1% (wt/vol) dodecyl maltoside (DM) (Anatrace, Maumee, Ohio) in a buffer containing 50 mM Tris-HCl (pH 9.0), 30 mM KCl, 2 mM EDTA, and 10% (wt/vol) glycerol in the presence of the protease inhibitors listed above (14). Solubilized proteins were loaded directly onto a DEAE-Sepharose 6B-CL (Pharmacia) anion-exchange column equilibrated with 30 mM KCl–50 mM Tris-HCl (pH 9.0)–2 mM EDTA–0.1 mM PMSF–0.01% (wt/vol) DM–10% glycerol. After extensive washes with this buffer, the pH of the washing solution was decreased to 8.0, and cyt c_y was eluted in two steps with 100 and 150 mM KCl in the above-described buffer. The 100 mM KCl fraction contained the majority of cyt c_y, as judged by dot blot assays using monoclonal antibody M2, which specifically recognizes the FLAG epitope. This fraction was concentrated using Centriprep 50 units (50-kDa molecular mass cutoff limit; Amicon), while the 150 mM KCl elution fraction was discarded. The concentrated sample was dialyzed overnight against 50 mM Tris-HCl (pH 7.4)–150 mM NaCl (TBS buffer) and applied to a monoclonal antibody M2 affinity column (bed volume, 1.8 ml). The column was washed extensively (approximately 40 bed volumes) in TBS buffer with 0.01% DM, and FLAGed cyt c_y was eluted with 0.1 M glycine-HCl (pH 3.0) buffer containing 0.01% DM. Fractions (1 ml each) were collected directly into tubes containing 100 μl of 1 M Tris-HCl (pH 8.0), and those fractions containing FLAGed cyt c_y were pooled, dialyzed against TBS buffer containing 10% glycerol, concentrated as described above, and stored at −80°C. In a typical experiment, from 10 g (wet weight) of cells of pHM7/FJ2, approximately 200 mg of solubilized membrane proteins and 0.5 mg of >95% pure cyt c_y (estimated by densitometric traces of Coomassie brilliant blue-stained SDS-PAGE gels) was obtained after DEAE–anion-exchange and anti-FLAG affinity chromatography.

SDS-PAGE, Western, and dot blot analyses. SDS-PAGE was performed as described elsewhere (37) with 16.5 or 10% polyacrylamide gels. Samples were solubilized in 2% SDS–5% β-mercaptoethanol and incubated either for 15 min at 75°C for Coomassie staining and Western blots or for 5 min at 37°C for visualization of *c*-type cytochromes with 3,3',5,5'-tetramethylbenzidine (TMBZ) (41). Western and dot blot analyses used the M2 antibody (5 μg/ml) that recognizes a carboxyl-terminus-located FLAG epitope (Scientific Imaging Systems, Kodak). Immunocomplexes were detected by using horseradish peroxidase-conjugated goat anti-mouse secondary antibodies (Boehringer Mannheim), and diaminobenzidine was used as a peroxidase substrate enhanced with $NiCl_2$.

Spectroscopic analysis. Optical difference spectra of purified cyt c_y (ascorbate reduced minus ferricyanide oxidized) were taken as previously described (14), and the concentrations of the *c*-type cytochromes were estimated from the reduced minus the oxidized spectra, using an absorption coefficient $\varepsilon_{550\text{-}540}$ of 20.0 mM^{-1} cm^{-1}. Potentiometric equilibrium titration of the heme group of cyt c_y was carried out as described by Dutton (9), and an $E_{m,7}$ for cyt c_y was deduced by fitting normalized absorbance differences (A_{551} minus A_{540}) to a single $n = 1$ Nernst equation.

Amino acid sequencing of cyt c_y and determination of its molecular weight by electrospray mass spectroscopy. Amino acid sequence analysis of purified cyt c_y was performed by automated Edman degradation using an Applied Biosystems model 470A sequencer run according to the manufacturer's specifications as described elsewhere (14). After SDS-PAGE and electroblotting of the sample to a polyvinylidene difluoride membrane, protein bands present were visualized using Coomassie brilliant blue, and cyt c_y identified by anti-FLAG M2 antibody was either subjected directly to N-terminal amino acid sequencing or treated with trypsin. Peptides resulting from trypsin treatment were separated by high-pressure liquid chromatography (HPLC) and then sequenced.

Electrospray mass spectrometry was performed with a VG 30-250 quadrupole mass spectrometer equipped with the manufacturer's electrospray source (Fisons Instruments). Spectral data were acquired over an *m/z* range of 600 to 1,600/10 s. On-line HPLC purification of cyt c_y was done using a Waters prototype capillary HPLC system with a capillary column (dimensions, 300 μm [inside diameter] by 15 cm) obtained from LC Packings (Amsterdam, The Netherlands) and used with a flow rate of 2.1 μl/min. The mobile phase consisted of 0.12% trifluoroacetate (solvent A), and acetonitrile-water (95/5) with 0.1% trifluoroacetate (solvent B). After injection of the sample, the column was washed with solvent A for 15 min and then by a gradient of solvent B (0 to 100%) for 20 min.

Chemicals. All chemicals, unless otherwise noted, were of reagent grade and were obtained from commercial sources. Redox mediators were purchased as described elsewhere (14), and *n*-dodecyl β-D-maltoside was from Anatrace.

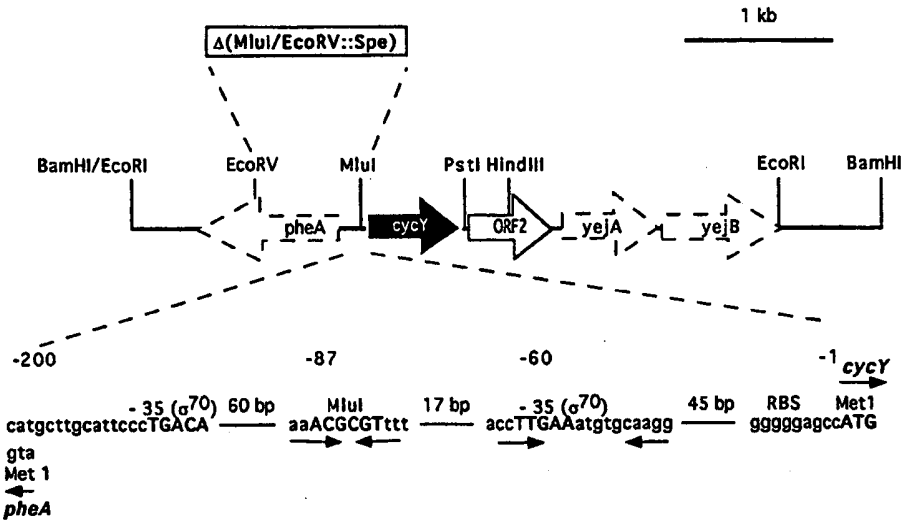

FIG. 1. Physical and genetic maps of the chromosomal region surrounding *cycY* indicate that this gene is monocistronic. Δ(*MluI*/*Eco*RV::Spe), indicating the chromosomal deletion in strains FJ5 and FJ6, is shown upstream of *cycY*. Also indicated are some features of the *pheA-cycY* intergenic region, shown to be sufficient to govern the synthesis of the promoterless *lacZ* under respiratory and Ps growth conditions. RBS, ribosome binding site; −35 (σ^{70}), putative −35 region(s) of the *cycY* promoter. Arrows indicate the secondary structures observed.

RESULTS

Physical organization of genes surrounding *cycY* of *R. capsulatus*. *R. capsulatus cycY* was previously mapped to the cosmid 2C8 of the ordered cosmid library of this organism (12). Determination of the DNA sequence immediately upstream of *cycY* revealed the presence of an open reading frame (ORF) homologous to the chorismate mutase/prephenate dehydratase gene (*pheA*) of several bacterial species (11). This enzyme converts chorismate to prephenate, a precursor for phenylalanine and tyrosine biosynthesis (44). To establish the function of this ORF, the approximately 900-bp *Mlu*I/*Eco*RV DNA fragment upstream of *cycY* (Fig. 1) was inactivated by interposon mutagenesis using a gene transfer agent as described in Materials and Methods. The resulting mutant, FJ5, grew well on enriched medium under Ps and respiratory (Res) growth conditions but was unable to do so on minimal growth medium unless phenylalanine was added as a supplement. This finding confirmed that this ORF is involved in the biosynthesis of aromatic amino acids, so it was named *pheA* in agreement with its homologs in other bacterial species (Fig. 1). In addition, since pFJ62 carrying the 2.0-kb *Mlu*I/*Bam*HI fragment upstream of *cycY* complemented FJ5 to prototrophy, it was concluded that the entire *pheA* must be contained within this fragment of DNA (18).

Unexpectedly, FJ6, which is an otherwise isogenic cyt c_2^- derivative of FJ5, was unable to grow by Ps on enriched medium or on minimal medium supplemented with phenylalanine. Considering that *Mlu*I/*Eco*RV deletion leaves *cycY* intact and that the adjacent *Mlu*I/*Pst*I fragment complements FJ2 (cyt c_2^- c_y^-) for Ps^+ growth when carried by a multicopy plasmid such as pFJ63 (Fig. 1) (18), it is not clear why FJ6 carrying an intact chromosomal copy of *cycY* is Ps^- unless the region surrounding the *Mlu*I site affects its regulation (Fig. 1). That the *pheA-cycY* intergenic region upstream of *cycY* indeed contains the expression region of *cycY* was confirmed by its fusion to a promoterless *lacZ* reporter gene. *R. capsulatus* MT-1131, which contains this construct, yielded blue colonies on X-Gal (5-bromo-4-chloro-3-indolyl-β-D-galactopyranoside) plates under aerobic and Ps growth conditions (data not shown). The molecular basis for the effect of a Δ(*Mlu*I-*Eco*RV) mutation on *cycY* regulation is currently under study and will be reported elsewhere.

Neither the function of ORF2 immediately downstream of *cycY* nor the functions of the ORFs following it (homologs of *E. coli yejA* and *yejB*, encoding a hypothetical ABC-type ATP-dependent transport operon) are currently known. Moreover, their insertional inactivation has no detectable effect on Ps^+ or Res^+ growth of a wild-type *R. capsulatus* strain or of its cyt c_2^- derivative. Therefore, these ORFs are apparently not essential for Ps electron transport in this species under the growth conditions used. Finally, note that the overall genetic organization of the genes surrounding *cycY* (Fig. 1) is conserved between *R. capsulatus* and *R. sphaeroides* (49).

Translational initiation of *R. capsulatus cycY*. The N-terminal region of *cycY* contains five ATG codons (corresponding to residues Met-1, -6, -13, -38, and -70 of ORF1) (18) that could each possibly serve as its initiator codon. Of these, Met-1, -13, and -70, which are preceded by ribosome binding-like sequences, were replaced with leucine by site-directed mutagenesis, and the resulting mutants were tested for their abilities to produce cyt c_y and complement FJ2 to a Ps^+ growth phenotype (data not shown). Of these substitutions, only Met13Leu completely abolished the production of cyt c_y, suggesting that the corresponding codon is the likely translation initiator of *cycY*. That this methionine is indeed the first amino acid of cyt c_y was confirmed by N-terminal amino acid sequencing of purified cyt c_y (see below), and hereafter, it was used as position 1 to number the amino acids of cyt c_y. Accordingly, *cycY* encodes a protein of 199 amino acids with a calculated molecular mass of 20.6 kDa for the apoprotein, and its first 28 residues form a prokaryotic signal sequence-like motif (34) (Fig. 2).

Cellular localization and topology of cyt c_y. To establish that cyt c_y is indeed an integral membrane protein, membrane sheets isolated from *R. capsulatus* MT-1131 were first treated either with an alkaline buffer (pH 10.5) or a chaotropic agent (1 M NaBr) as described in Materials and Methods. Neither one of these treatments removed cytochrome c_y or c_1 of the cyt bc_1 complex from the membrane (data not shown). Since cyt c_1

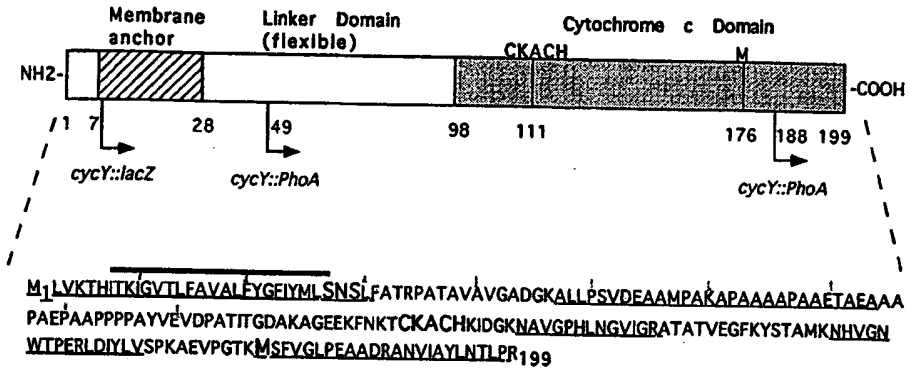

FIG. 2. The primary structure of cyt c_y (M1 corresponds to the translational initiator of *cycY* as determined in this study) indicates that it has three different domains. The carboxy-terminal domain of cyt c_y, which is highly homologous to mitochondrial *c*-type cytochromes (18), is fused to a relatively long (98-residue) amino-terminal extension. The latter domain can further be divided into a combined signal sequence and a membrane anchor (residues 1 to 28) which is connected to the cyt *c* domain by a 70-amino-acid-long, presumably flexible linker region. The predicted alpha-helical region (residues 7 to 28) is indicated by a line drawn above these residues. Underlined residues indicate those determined directly by amino acid sequencing with purified FLAGed cyt c_y and its tryptic digest fragments. A putative cleavage site for the signal sequence (residues SNS at positions 28 to 30), a heme binding consensus sequence (CxyCH at positions 112 to 116), and a fully conserved axial ligand (M at position 176) of the heme group are indicated in boldface type. Also shown are the positions of the *cycY::phoA* and *cycY::lacZ* fusions isolated during this work.

is a known integral membrane protein, it was therefore concluded that cyt c_y must also be one.

Next, to probe whether the cyt *c* domain of cyt c_y is facing toward the periplasm, as suggested by its electron carrier function, two *cycY::phoA* fusions located at residues 49 and 188 of cyt c_y (Fig. 2) were obtained as described earlier. These in-frame fusions produced active alkaline phosphatases, which indicated that the amino acid residues located at least beyond position 49 of cyt c_y were translocated to the periplasm (25). Moreover, various computer programs designed to predict the membrane topology of proteins identified only one putative membrane-spanning helix in cyt c_y (between residues 7 and 28 and overlapping with its signal sequence). We therefore concluded that cyt c_y must be anchored to the membrane by this helix, leaving a short N-terminal extension in the cytoplasm.

Purification and biochemical characterization of cyt c_y. Next, isolation of cyt c_y was necessary in order to define its physicochemical properties as well as to investigate its mode of membrane attachment. Since the amount of cyt c_y in cells is limited, an epitope-tagged version of it was prepared to aid in its purification. The C-terminal ends of class I cyt *c* usually extend away from the core part of the protein, allowing them to be extended by additional residues (27). Thus, an epitope-tagged derivative of cyt c_y was constructed by fusing the highly antigenic FLAG epitope to the C-terminal end of cyt c_y. The resulting FLAGed cyt c_y was produced in a biologically active form in both *R. capsulatus* FJ2 (cyts c_2^- c_y^-) and *R. sphaeroides* Gadc$_2$ (cyt c_2^-) and was able to complement for Ps$^+$ growth both of these mutants with an efficiency comparable to that of its wild-type counterpart (data not shown). TMBZ/SDS-PAGE (heme staining) and Western blot analyses of strains producing FLAGed cyt c_y revealed that among the membrane-associated TMBZ-stained bands, only that of 29 kDa was shifted to an apparent molecular mass of ≈31 kDa. This band, which is eliminated when *cycY* is deleted, was also recognized with anti-FLAG antibodies and was therefore identified positively as the mature and functional form of cyt c_y (Fig. 3A and B).

The FLAGed cyt c_y, purified from DM-solubilized chromatophore membranes by immunoaffinity chromatography, ran as a single polypeptide on SDS-PAGE gels with the Tris/Tricine gel system (Fig. 3C) if the sample was treated at 75°C in SDS-loading buffer for 15 min prior to loading. However, when denaturation was carried out at 37°C instead of 75°C, two major bands of 26 and 31 kDa were observed (not shown). This indicated that, like many membrane proteins, cyt c_y runs as multiple forms on SDS-PAGE gels and explained why the deletion of *cycY* was previously found to correlate with the elimination of more than one TMBZ-stained band (18).

The ascorbate-reduced absolute spectrum of purified cyt c_y has symmetric absorption maxima at 551, 521, and 417 nm, while the ferricyanide-oxidized absolute spectrum has a maximum at 409 nm (Fig. 4A). These values are similar to those of many mitochondrial class I *c*-type cytochromes which have the Cys-Xaa-Yaa-Cys-His heme-binding motif and a distal methi-

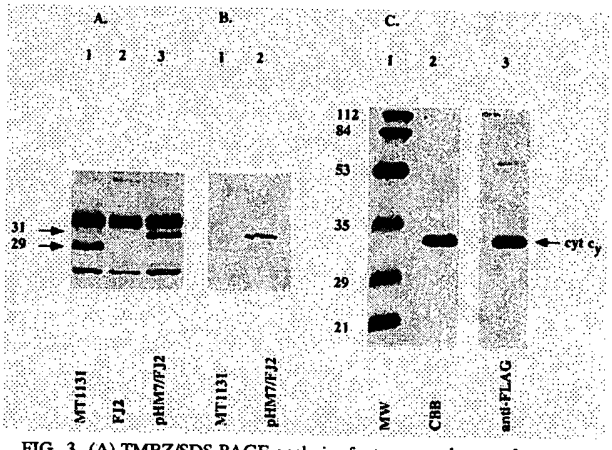

FIG. 3. (A) TMBZ/SDS-PAGE analysis of *c*-type cytochromes from various *R. capsulatus* strains obtained from cells grown on enriched MPYE medium (300 μg of membrane proteins were loaded per lane). Lane 1, MT-1131 (wild type); lane 2, FJ2 (cyt c_2^- cyt c_y^-); lane 3, pHM7/FJ2 (FLAGed cyt c_y). Note that the addition of the FLAG epitope increases the apparent mass of cyt c_y by approximately 2 kDa. (B) Western blot analysis using anti-FLAG M2 antibody (5 μg/ml). After electrophoretic transfer of proteins onto a polyvinylidene difluoride membrane, FLAGed cyt c_y was detected with horseradish peroxidase-conjugated secondary antibody with $NiCl_2$-enhanced 3,3′-diaminobenzidine as the substrate. Lane 1, MT-1131; lane 2, pHM7/FJ2. (C) SDS-PAGE analysis and immunoblot of isolated cyt c_y. Lane 1 corresponds to prestained molecular mass (MW) markers (BioRad) in kilodaltons. Lane 2 contains 6.6 μg of purified protein stained with Coomassie brilliant blue (CBB), and the protein band (≈31 kDa) present in this sample can also be recognized with anti-FLAG antibody (lane 3, 2.1 μg of protein).

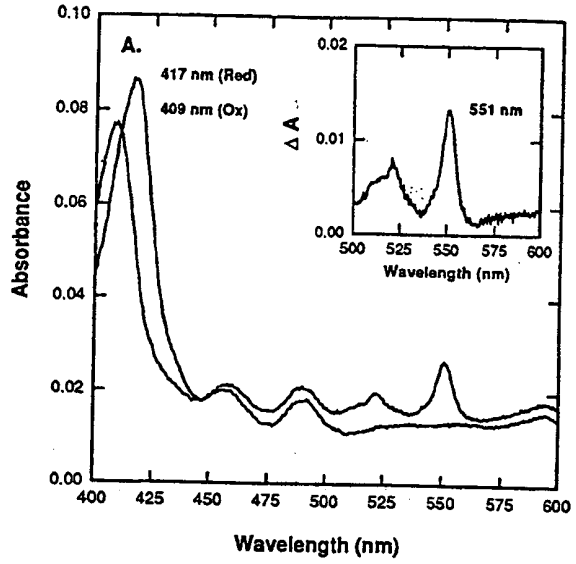

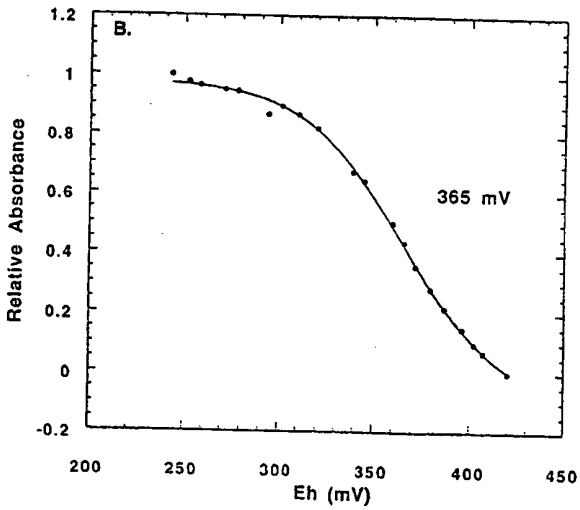

FIG. 4. (A) The ascorbate-reduced absolute spectrum of FLAGed cyt c_y shows maxima at 551, 521, and 417 nm, while its oxidized spectrum has a maximum at 409 nm. The ascorbate-reduced minus ferricyanide-oxidized spectrum of cyt c_y is shown in the inset. All spectra were recorded in 50 mM Tris-HCl (pH 8.0) in the presence of 0.01% (wt/vol) DM. The concentration of cyt c_y was approximately 1 μM. (B) Potentiometric equilibrium redox titration of cyt c_y fitted to a single $n = 1$ Nernst equation indicates that cyt c_y has a redox midpoint ($E_{m,7}$) of 365 mV. The titration was performed in 100 mM KCl–20 mM morpholinepropanesulfonic acid (MOPS)-OH (pH 7.0) in the presence of 0.01% DM. Redox mediators were as described elsewhere (9, 14).

onine residue as the sixth ligand of the heme iron (27). Although the so-called "charge transfer band" at approximately 695 nm that is indicative of this distal Met ligand is not visible in the optical spectra of purified protein (probably because of the low concentration of cyt c_y used), all the liganding residues are conserved in cyt c_y according to alignments of its sequence with mitochondrial cyt *c* such as those from horse heart and tuna (Fig. 2). Finally, potentiometric equilibrium titration of the heme group of cyt c_y indicated that its $E_{m,7}$ is around +365 mV in the presence of 100 mM KCl at pH 7.0 (Fig. 4B). This value is approximately 100 mV more positive than that of the equine cyt *c* but is practically identical to that of cyt c_2 from phototrophs, including *R. capsulatus*. It is also in excellent agreement with the values previously determined using chromatophores of *R. capsulatus* mutant MT-GS18 lacking both cyt c_2 and cyt c_1 (31, 48). Thus, the thermodynamic properties of the membrane-bound cyt c_y are similar to those of cyt c_2 both in membranes (in situ) and in the purified state (in vitro).

Cyt c_y is anchored to the membrane by its unprocessed N-terminal helix. One of the purposes behind the purification of cyt c_y was to determine whether its signal sequence-like N-terminal portion is processed during its translocation into the periplasm. The N-terminal amino acid sequence obtained using purified cyt c_y and shown in Fig. 2 confirmed the translational start site inferred by the site-directed mutagenesis experiments described earlier and indicated that the mature form of cyt c_y is not processed. To eliminate the possible presence of any major posttranslational modification in cyt c_y, purified protein was also subjected to electrospray mass spectrometry. This analysis (data not shown) indicated a molecular mass of 22,299 ± 5.7 Da for purified cyt c_y, which is only 11 Da higher than the calculated molecular mass of the FLAGed version of holo cyt c_y (22,288 Da). The small difference, which could be due to some minor modifications such as the methylation of a lysine residue at an unknown position, is consistent with the lack of any N-terminal processing during the maturation of cyt c_y. Moreover, it clearly is not compatible with the posttranslational addition of a diacyl fatty acid or other, larger fatty acids known to serve as membrane anchors for some cytochromes such as cyt c_{551} of the thermophilic bacterium PS3 (13) or the tetraheme cyt *c* subunit of the *Rhodopseudomonas viridis* RC (46).

The N-terminal domain of *R. capsulatus* cyt c_y is sufficient to anchor the periplasmic cyt c_2 to the membrane. On the basis of the overall findings described above, we reasoned that if the N-terminal extension of cyt c_y indeed anchors it to the membrane, then it should also be able to do that for a known periplasmic electron carrier such as cyt c_2. This prediction was tested by creating a hybrid cyt *c* formed of the N-terminal extension of cyt c_y and the mature form of cyt c_2, as described in Materials and Methods and the legend to Fig. 5A. The resulting chimeric cyt, MA-c_2, complemented FJ2 (cyts c_2^- c_y^-) and Gadc$_2$ (cyt c_2^-) to a Ps^+ growth phenotype, and immunoblot analyses of the membrane sheets derived from the former strain by using polyclonal antibodies against cyt c_2 demonstrated that cyt MA-c_2 remained membrane attached (Fig. 5B). This finding established that the N-terminal extension of cyt c_y is sufficient to anchor cyt c_2 to the membrane. Further, since the Ps doubling time (153 ± 16 min) on enriched MPYE medium of pHM8/FJ2 carrying this chimera is comparable to that of the *R. capsulatus* mutant FJ1 lacking cyt c_y (133 ± 11 min under identical conditions) (18), then this membrane-anchored form of cyt c_2 apparently supports Ps^+ growth as efficiently as its soluble wild-type counterpart does. On the other hand, the hybrid cyt S-c_y (where the N-terminal extension of cyt c_y is deleted) was unable to do so and was not further investigated.

DISCUSSION

In this work, the *R. capsulatus* membrane-attached electron carrier cyt c_y, formed of a cyt *c* domain preceded by an approximately 100-amino-acid-long N-terminal anchor-linker domain (Fig. 2) and its structural gene, *cycY*, were studied in detail. First, the initiator codon of *cycY* and the cellular loca-

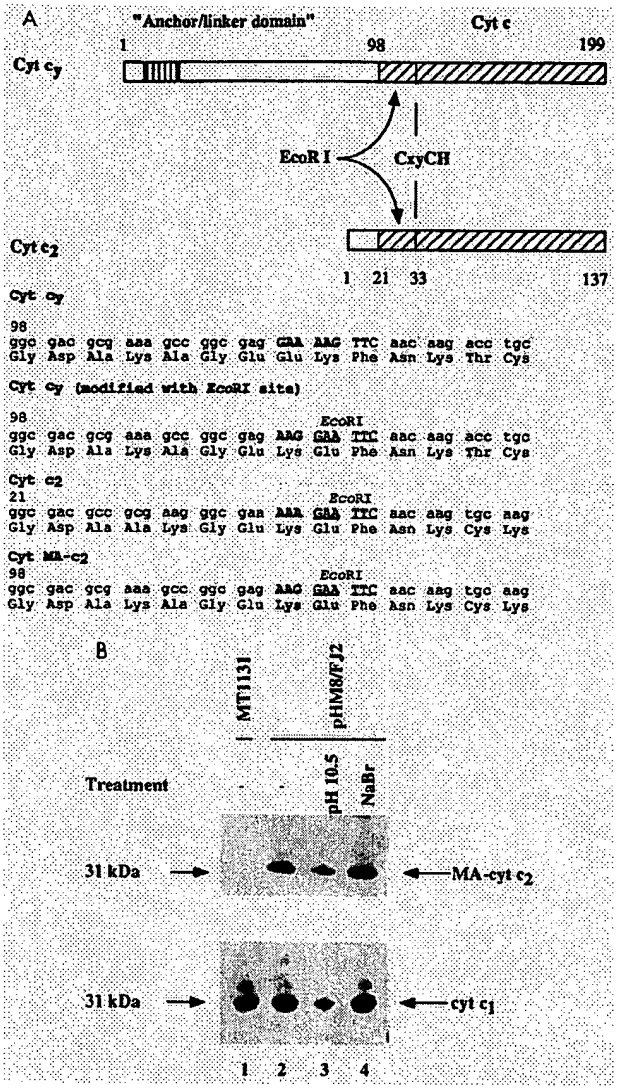

FIG. 5. (A) Domain swapping between the cyts c_2 and c_y. Using either an existing (i.e., cyt c_2) or a created (i.e., cyt c_y) *Eco*RI site, cyt c_2 was fused in frame to the N-terminal subdomain of cyt c_y. The resulting chimeric cyt (cyt MA-c_2), with a calculated molecular mass of 22.1 kDa, is able to complement FJ2 (cyt c_2^- c_y^-) to a Ps^+ phenotype. Also shown are the partial amino acid sequences of cyts c_y, c_2, and MA-c_2 at the fusion joint. (B) Western blot analysis (using SDS–10% PAGE) of membrane sheets isolated from *R. capsulatus* MT-1131 (wild type) and pHM8/FJ2 (cyt MA-c_2) treated as described in Materials and Methods. (Top panel) Samples containing approximately 5 μg of membrane proteins were probed with polyclonal antibody against *R. capsulatus* cyt c_2 (32). Note that under the conditions used here for sample preparation, the periplasmic cyt c_2 does not remain associated with the membrane fragments of MT-1131 (lane 1), while cyt MA-c_2 cannot be removed from membranes by using alkaline pH and chaotropic agents (lanes 2 through 4). (Bottom panel) The same samples were also probed with antibodies against cyt c_1 of the cyt bc_1 complex as a control. Note that cyt MA-c_2 runs on SDS-PAGE like cyt c_1 with an M_r of 31 kDa (see also Fig. 3A).

tion of cyt c_y were defined by using site-directed mutagenesis and *phoA* fusions. Mutational analysis indicated that the *R. capsulatus cycY*, like that of *R. sphaeroides*, is surrounded by genes that are not required for Ps. The finding that a *cycY::lacZ* fusion carrying the 5′ upstream *pheA-cycY* intergenic region was able to produce an active β-galactosidase indicated that the promoter(s) of *cycY* must be located in this region. Note that there are two putative σ^{70}-like −35 sequences situated 65 and 185 bases upstream of the translational start site of *cycY* that are separated by the *Mlu*I site used to create the Δ(*Mlu*I/*Eco*RV::Spe) mutation (Fig. 1). The first 90 bp of this region, extending from the ATG start codon of *cycY* to the *Mlu*I site, is able to direct the synthesis of enough cyt c_y to support Ps^+ growth of *R. capsulatus* FJ2 (cyts c_2^- and c_y^-) when it is present in multiple copies (i.e., pFJ63) (18) but not in a single copy (i.e., FJ6). Thus, whether multiple and possibly differentially regulated *cycY* promoters govern the expression of cyt c_y, as is the case for *R. sphaeroides* cyt c_2 (24), is an intriguing issue for future studies.

During this work, cyt c_y protein was purified to homogeneity by affinity chromatography after its carboxyl terminus had been tagged with the FLAG epitope. The overall data obtained using purified material established that the N-terminal domain of cyt c_y is unprocessed during its translocation to the periplasm, leaving it anchored to the membrane. This domain was also sufficient to anchor the periplasmic cyt c_2 into the lipid bilayer, yielding a functional chimeric cyt MA-c_2. Future analysis of the electron transfer properties of cyt MA-c_2 and its comparison to the soluble cyt c_2 should yield extremely valuable information on how anchoring an electron carrier to the membrane affects its electron transfer properties. It was observed that the purified FLAGed derivative of cyt c_y runs on SDS-PAGE with an apparent molecular mass of 31 kDa in contrast to its actual molecular mass of 22.3 kDa as determined by mass spectrometry. This anomalous migration behavior appears to be caused by the N-terminal domain of cyt c_y, since the apparent molecular mass of cyt MA-c_2 formed from this domain and cyt c_2 was also 31 kDa (instead of its calculated mass of 22.1 kDa) (Fig. 5).

Earlier experiments performed using chromatophores have suggested an α peak maximum of 551 to 552 nm (reduced minus oxidized) and an $E_{m,7}$ of ≈345 to 360 mV for the native cyt c_y (19, 21, 33, 48). The properties of the purified FLAGed derivative of cyt c_y are in close agreement with these values and are similar to those of cyt c_2, indicating that addition of the FLAG epitope does not drastically change the characteristics of cyt c_y. Thus, the different rates of electron transfer to the RC from cyt c_2 (approximately 250 μs) (19) and cyt c_y (less than 100 μs) (33) may be a reflection of their different modes of interaction with their redox partners. In particular, since the membrane association of cyt c_y necessarily limits its diffusion to the plane of the plasma membrane, it is not clear how it interacts with the RC, although the relatively long and flexible linker arm of cyt c_y may somehow facilitate the interaction (Fig. 2). At this point, the details of the physical interactions between the RC, cyt c_y, and the cyt bc_1 complex both in vivo (18) and in vitro are not well understood. Considering that the RC in Ps membranes might be surrounded by a ring of light-harvesting I complexes (22), the finding that cyt MA-c_2 can also support Ps^+ growth of FJ2 (cyt c_2^- c_y^-) is intriguing. Moreover, considering that the N-terminal domains of various homologs of cyt c_y have similar hydrophobicity profiles, it is not clear why some of them, like that of *R. sphaeroides*, are incapable of supporting Ps growth.

The earlier finding that on enriched MPYE medium the steady-state presence of cyt c_y in intracytoplasmic membranes is dependent on the presence of cyt bc_1 suggests a close interaction between these proteins (19). This situation is reminiscent of that described for *Saccharomyces cerevisiae*, in which increased degradation of cyt *c* in the absence of its physiological partners was seen (29). Note that for *P. denitrificans*, a supercomplex formed by the cyt bc_1 complex, cyt c_{552} (a homolog of cyt c_y), and the cyt aa_3 oxidase has been purified under specific conditions (3). Interestingly, the recent resolu-

tion of the three-dimensional structure of the *P. denitrificans* cyt aa_3 oxidase revealed that two helical bundles of subunit III form a cleft, possibly constituting a docking site for the membrane anchor of cyt c_{552} (17). Thus, the possibility that cyt c_y interacts closely with the RC and the cyt bc_1 complex to optimize electron transfer requires further attention.

Why bacteria like *R. capsulatus* have soluble and membrane-bound isoforms of cyt *c* to connect the cyt bc_1 complex to the RC or to cyt cbb_3 (15, 18) is not known. Yet, cyt c_y homologs have been encountered in *P. denitrificans* (43), *B. japonicum* (4), *Nitrobacter vinogradskyi* (28), *R. sphaeroides* (49), and possibly *Rhodospirillum rubrum* (27a). Their presence is also anticipated in many other phototrophic bacteria, especially in those apparently lacking the soluble electron carrier cyt c_2, such as members of the genera *Rhodoferax*, *Rhodocyclus*, *Chromatium*, *Ectothiorhodospira*, and *Heliobacterium* (26). Thus, it could be argued that electron transfer via cyt c_y to the RC is more efficient during multiple turnovers because of the lack of any diffusible periplasmic components (19, 33, 45). On the other hand, it is not known whether cyt c_2 and cyt c_y are used preferentially under yet to be determined specific growth conditions or whether two physically distinct pools of RC or cyt cbb_3 oxidase "committed" to interact with different electron carriers exist in various species, including *R. capsulatus*. Finally, note that cyt c_2 is also an essential electron carrier in vivo during anaerobic respiratory growth in the presence of nitrous oxide as an electron sink (35). In any event, clearly, *Rhodobacter* species continue to provide an attractive model system for understanding how the different electron carriers function to support maximal electron transport during various growth modes.

ACKNOWLEDGMENTS

This work was supported by grant 91ER20052 from the Department of Energy. H.M. acknowledges financial support from the Finnish Academy of Sciences and the Thanks to Scandinavia organization.

We thank B. Pramanik, S. Saribas, and S. Lang for their valuable help with electrospray mass spectroscopy, redox titrations, and DNA sequencing. λ Tn*phoA* and pXCA601 were kind gifts of D. Schifferli and C. Bauer, respectively. H.M. also thanks K. A. Gray and H.-G. Koch for valuable discussions during this work.

REFERENCES

1. **Adams, C. W., M. E. Forrest, S. N. Cohen, and J. T. Beatty.** 1989. Structural and functional analysis of transcriptional control of the *Rhodobacter capsulatus puf* operon. J. Bacteriol. **171**:473–482.
2. **Altschul, S. F., W. Gish, W. Miller, E. W. Myers, and D. J. Lipman.** 1990. Basic local alignment search tool. J. Mol. Biol. **215**:403–410.
3. **Berry, E. A., and B. L. Trumpower.** 1985. Isolation of ubiquinol oxidase from *Paracoccus denitrificans* and resolution into cytochrome bc_1 and cytochrome c-aa_3 complexes. J. Biol. Chem. **260**:2458–2467.
4. **Bott, M., D. Ritz, and H. Hennecke.** 1991. The *Bradyrhizobium japonicum cycM* gene encodes a membrane-anchored homolog of mitochondrial cytochrome *c*. J. Bacteriol. **173**:6766–6772.
5. **Caffrey, M., E. Davidson, M. Cusanovich, and F. Daldal.** 1992. Cytochrome c_2 mutants of *Rhodobacter capsulatus*. Arch. Biochem. Biophys. **292**:419–426.
6. **Daldal, F., S. Cheng, J. Applebaum, E. Davidson, and R. C. Prince.** 1986. Cytochrome c_2 is not essential for photosynthetic growth of *Rhodopseudomonas capsulata*. Proc. Natl. Acad. Sci. USA **83**:2012–2016.
7. **Ditta, G., T. Schmidhauser, E. Yakobson, P. Lu, X.-W. Liang, D. R. Finlay, D. Guiney, and D. R. Helinski.** 1985. Plasmids related to the broad host range vector, pRK290, useful for gene cloning and for monitoring gene expression. Plasmid **13**:149–153.
8. **Donohue, T. J., A. G. McEwan, D. S. Van, A. R. Crofts, and S. Kaplan.** 1988. Phenotypic and genetic characterization of cytochrome c_2 deficient mutants of *Rhodobacter sphaeroides*. Biochemistry **27**:1918–1925.
9. **Dutton, P. L.** 1978. Redox potentiometry: determination of midpoint potentials of oxidation-reduction components of biological electron-transfer systems. Methods Enzymol. **54**:411–435.
10. **Ferguson, S. J.** 1991. The functions and synthesis of bacterial c-type cytochromes with particular reference to *Paracoccus denitrificans* and *Rhodobacter capsulatus*. Biochim. Biophys. Acta **1058**:17–20.
11. **Fischer, R. S., G. Zhao, and R. A. Jensen.** 1991. Cloning, sequencing, and expression of the P-protein gene (*pheA*) of *Pseudomonas stutzeri* in *Escherichia coli*: implications for evolutionary relationships in phenylalanine biosynthesis. J. Gen. Microbiol. **137**:1293–1301.
12. **Fonstein, M., E. G. Koshy, T. Nikolskaya, P. Mourachov, and R. Haselkorn.** 1995. Refinement of the high-resolution physical and genetic map of *Rhodobacter capsulatus* and genome surveys using blots of the cosmid encyclopedia. EMBO J. **14**:1827–1841.
13. **Fujiwara, Y., M. Oka, T. Hamamoto, and N. Sone.** 1993. Cytochrome *c-551* of the thermophilic bacterium PS3, DNA sequence and analysis of the mature cytochrome. Biochim. Biophys. Acta **1144**:213–219.
14. **Gray, K. A., M. Grooms, H. Myllykallio, C. Moomaw, C. Slaughter, and F. Daldal.** 1994. *Rhodobacter capsulatus* contains a novel *cb*-type cytochrome *c* oxidase without a Cu_A center. Biochemistry **33**:3120–3127.
15. **Hochkoeppler, A., F. E. Jenney, S. E. Lang, D. Zannoni, and F. Daldal.** 1995. Membrane-associated cytochrome c_y of *Rhodobacter capsulatus* is an electron carrier from the cytochrome bc_1 complex to the cytochrome *c* oxidase during respiration. J. Bacteriol. **177**:608–613.
16. **Hofmann, K., and W. Stoffel.** 1993. TMbase—a database of membrane spanning protein segments. Biol. Chem. Hoppe-Seyler **347**:166.
17. **Iwata, S., C. Ostermeier, B. Ludwig, and H. Michel.** 1995. Structure at 2.8 Å resolution of cytochrome *c* oxidase from *Paracoccus denitrificans*. Nature **376**:660–669.
18. **Jenney, F. E., and F. Daldal.** 1993. A novel membrane-associated *c*-type cytochrome, cyt c_y, can mediate the photosynthetic growth of *Rhodobacter capsulatus* and *Rhodobacter sphaeroides*. EMBO J. **12**:1283–1292.
19. **Jenney, F. E., R. C. Prince, and F. Daldal.** 1994. Roles of the soluble cytochrome c_2 and membrane-associated cytochrome c_y of *Rhodobacter capsulatus* in photosynthetic electron transfer. Biochemistry **33**:2496–2502.
20. **Jenney, F. E., R. C. Prince, and F. Daldal.** 1996. The membrane-bound cytochrome c_y of *Rhodobacter capsulatus* can serve as an electron donor to the photosynthetic reaction center of *Rhodobacter sphaeroides*. Biochim. Biophys. Acta **1273**:159–164.
21. **Jones, M. R., A. G. McEwan, and J. B. Jackson.** 1990. The role of *c*-type cytochromes in the photosynthetic electron transport pathway of *Rhodobacter capsulatus*. Biochim. Biophys. Acta **1019**:59–66.
22. **Karrasch, S., P. A. Bullough, and R. Ghosh.** 1995. The 8.5 Å projection map of the light-harvesting complex I from *Rhodospirillum rubrum* reveals a ring composed of 16 subunits. EMBO J. **14**:631–638.
23. **Lowry, O., N. Rosebrough, A. Farr, and R. Randall.** 1951. Protein measurement with the Folin phenol reagent. J. Biol. Chem. **193**:265–275.
24. **MacGregor, B. J., and T. J. Donohue.** 1991. Evidence for two promoters for the cytochrome c_2 gene (*cycA*) of *Rhodobacter sphaeroides*. J. Bacteriol. **173**: 3949–3957.
25. **Manoil, C., and J. Beckwith.** 1986. A genetic approach to analyzing membrane protein topology. Science **233**:1403–1408.
26. **Meyer, T., and T. Donohue.** 1995. Cytochromes, iron-sulfur and copper proteins mediating electron transfer from the Cyt bc_1 complex to photosynthetic reaction center complexes, p. 725–745. *In* R. E. Blankenship, M. T. Madigan, and C. E. Bauer (ed.), Anoxygenic photosynthetic bacteria. Kluwer Academic Publishers, Norwell, Mass.
27. **Moore, G. R., and G. W. Pettigrew.** 1990. Cytochromes *c*—evolutionary, structural and physicochemical aspects. Springer-Verlag, Berlin.

27a. **Myllykallio, H., et al.** Unpublished data.

28. **Nomoto, T., Y. Fukumori, and T. Yamanaka.** 1993. Membrane-bound cytochrome *c* is an alternative electron donor for cytochrome aa_3 in *Nitrobacter winogradskyi*. J. Bacteriol. **175**:4400–4404.
29. **Pearce, D. A., and F. Sherman.** 1995. Diminished degradation of yeast cytochrome *c* by interactions with its physiological partners. Proc. Natl. Acad. Sci. USA **92**:3735–3739.
30. **Pfennig, N.** 1978. General physiology and ecology of photosynthetic bacteria, p. 3–14. *In* R. K. Clayton and W. R. Sistrom (ed.), The photosynthetic bacteria. Plenum Press, New York.
31. **Prince, R., and F. Daldal.** 1987. Physiological electron donors to the photochemical reaction center of *Rhodobacter capsulatus*. Biochim. Biophys. Acta **894**:370–378.
32. **Prince, R. C., A. Baccarini-Melandri, G. A. Hauska, B. A. Melandri, and A. R. Crofts.** 1975. Asymmetry of an energy transducing membrane: the location of cytochrome c_2 in *Rhodopseudomonas sphaeroides* and *Rhodopseudomonas capsulata*. Biochim. Biophys. Acta **387**:212–227.
33. **Prince, R. C., E. Davidson, C. E. Haith, and F. Daldal.** 1986. Photosynthetic electron transfer in the absence of cytochrome c_2 in *Rhodopseudomonas capsulata*: cytochrome c_2 is not essential for electron flow from the cytochrome bc_1 complex to the photochemical reaction center. Biochemistry **25**: 5208–5214.
34. **Pugsley, A. P.** 1993. The complete general secretory pathway in Gram-negative bacteria. Microbiol. Rev. **57**:50–108.
35. **Richardson, D. J., L. C. Bell, A. G. McEwan, J. B. Jackson, and S. J. Ferguson.** 1991. Cytochrome c_2 is essential for electron transfer to nitrous oxide reductase from physiological substrates in *Rhodobacter capsulatus* and can act as an electron donor to the reductase in vitro. Correlation with photoinhibition studies. Eur. J. Biochem. **199**:677–683.

36. **Sambrook, J., E. F. Fritsch, and T. Maniatis.** 1989. Molecular cloning: a laboratory manual. Cold Spring Harbor Laboratory Press, Cold Spring Harbor, N.Y.
37. **Schägger, H., and G. von Jagow.** 1987. Tricine-sodium dodecyl sulfate polyacrylamide gel electrophoresis for the separation of proteins in the range from 1 to 100 kDa. Anal. Biochem. **166**:368–379.
38. **Schifferli, D. M.** 1995. Use of Tn*phoA* and T7 RNA polymerase to study fimbrial proteins. Methods Enzymol. **253**:242–258.
39. **Scolnik, P., M. Walker, and B. Marrs.** 1980. Biosynthesis of carotenoids derived from neuosporene in *Rhodopseudomonas capsulata*. J. Biol. Chem. **255**:2427–2432.
40. **Sistrom, W.** 1960. A requirement for sodium in the growth of *Rhodopseudomonas sphaeroides*. J. Gen. Microbiol. **22**:778–785.
41. **Thomas, P. E., D. Ryan, and W. Levin.** 1976. An improved staining procedure for the detection of the peroxidase activity of cytochrome P-450 on sodium dodecyl sulfate polyacrylamide gels. Anal. Biochem. **75**:168–176.
42. **Thompson, J., D. Higgins, and T. Gibson.** 1994. CLUSTAL W: improving the sensitivity of progressive multiple sequence alignment through sequence weighting, positions-specific gap penalties and weight matrix choice. Nucleic Acids Res. **22**:4673–4680.
43. **Turba, A., M. Jetzek, and B. Ludwig.** 1995. Purification of *Paracoccus denitrificans* cytochrome c_{552} and sequence analysis of the gene. Eur. J. Biochem. **231**:259–265.
44. **Umbarger, H. E.** 1978. Amino acid biosynthesis and its regulation. Annu. Rev. Biochem. **47**:533–606.
45. **Vermeglio, A., P. Joliot, and A. Joliot.** 1995. Organization of electron transfer components and supercomplexes, p. 279–295. *In* R. E. Blankenship, M. T. Madigan, and C. E. Bauer (ed.), Anoxygenic photosynthetic bacteria. Kluwer Academic Publishers, Norwell, Mass.
46. **Weyer, K. A., W. Shafer, F. Lottspeich, and H. Michel.** 1987. The cytochrome subunit of the photosynthetic reaction center from *Rhodopseudomonas viridis* is a lipoprotein. Biochemistry **26**:2909–2914.
47. **Yen, H. C., N. T. Hu, and B. L. Marrs.** 1979. Characterization of the gene transfer agent made by an overproducer mutant of *Rhodopseudomonas capsulata*. J. Mol. Biol. **131**:157–168.
48. **Zannoni, D., G. Venturoli, and F. Daldal.** 1992. The role of the membrane cytochromes of *b*- and *c*-type in the electron transport chain of *Rhodobacter capsulatus*. Arch. Microbiol. **157**:367–374.
49. **Zeilstra-Ryalls, J. H., and S. Kaplan.** 1995. Aerobic and anaerobic regulation in *Rhodobacter sphaeroides* 2.4.1: the role of the *fnrL* gene. J. Bacteriol. **177**:6422–6431.